Analytical Methods

Accepted Manuscript

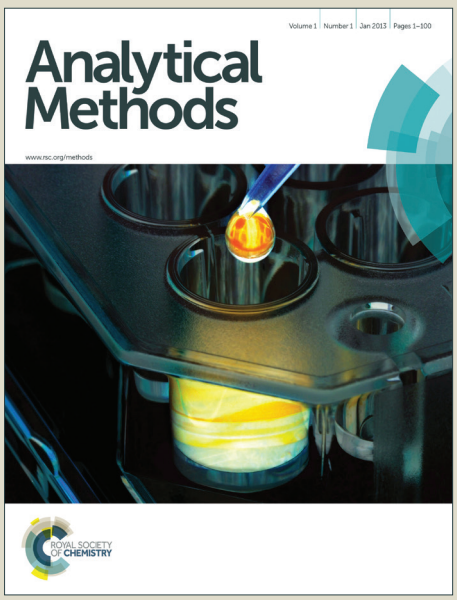

ROYAL SOCIETY OF CHEMISTRY

www.rsc.org/methods

Journal Name

RSCPublishing

COMMUNICATION

Electrospun micro/nano fibrous mesh based nontoxic sensor for optical detection of high humidity

Cite this: DOI: 10.1039/xoxxoooooox

Tianyu Wang, Hongxia, Fu, Xinrui Duan*, Zhengping Li*

Received ooth January 2012,
Accepted ooth January 2012

DOI: 10.1039/xoxxoooooox

www.rsc.org/

Optical transition of polyethylene oxide electrospun micro/nano fibrous mesh from opaque to transparent has been studied by UV-Vis spectroscopy and scanning electron microscopy. This transition occurs only above approximate 88% relative humidity and could use for humidity monitoring by naked eyes for food quality control in which low toxicity and irreversibility are highly required.

Humidity sensors are of great demand in many applications, such as food and pharmaceuticals quality monitoring, air conditioning systems, and medical equipment.[1] Lots efforts have been made to develop humidity sensors with different sensing mechanisms, such as electrical[2] and optical[3] detection. Humidity have great impact on germination of microorganism in food.[4] Especially when humidity is higher than approximate 85% ~ 90%, moulds and yeasts that frequently infest cereals and rice are significantly increased.[5] An effective humidity sensor for foods should be able to mark whether they have been exposed to critical humidity levels during their storage or not, regardless of current humidity levels. Namely, an irreversible humidity sensor. A safe, equipment-free, irreversible, and cheap sensor that could possibly place on each package of rice or cereals will help us to identify the risk before using.

Compare with electrical measurement based methods, colorimetric detection based sensors are usually cheap and does not require equipment. Color change of cobalt (II) chloride salt under different humidity have been used as test paper format in semiconductor packaging and desiccant monitoring due to its low cost. Mutagenicity and carcinogenicity cobalt chloride have been reported.[6a] Due to its relative low toxicity, copper chloride salt has been used to manufacture cobalt-free humidity indicator cards. Direct contact with copper chloride still can cause acute toxicity, skin irritation, and serious eye damage. Thus these metal chlorides salt based sensors are not ideal when low toxicity is required.[6b, c] Photonic crystal sensors have highly sensitive optical response to changes of humidity, unfortunately, most still are reversible sensors.[7]

Electrospinning is a simple and efficient tool to fabricate micro/nano fibrous membrane, and it has been widely used in tissue engineering and gas molecules sensing.[8] Large surface area of electrospun fibrous mesh makes it good platform for gaseous analyte detection.[9] Usually, a "sensing element" need to be doped into fibers or modified onto fiber surface to achieve detection.[10] As far as we know, by exploring the optical properties of electrospun micro/nano fibers for detecting purpose has not been reported yet.

It is well known that homogenous thin film of many polymers, for example polystyrene, Poly(methyl methacrylate), and polyethylene oxide (PEO) is almost visible transparent and the corresponding electrospun fibrous mesh is opaque due to light scattering at the greatly increased air/fiber interface. In the vapor of appropriate solvent, fibers should be gradually fuse to each other and eventually form a homogenous thin film, and opaque fibrous mesh will become transparent. Apparently it will be an irreversible process.

In this work, we chose water soluble and nontoxic polymer polyethylene oxide (PEO) to develop a safe and irreversible humidity sensor based on above mechanism. PEO is well-known as low toxic

polymer and has been used in pharmaceuticals, skin cream, and toothpastes, even used as food additives.[11] Resulted opaque electrospun fiber mesh became transparent in 10 min under high relative humidity environment. Later we used scanning electron microscopy imaging to investigate the change of morphology of fibrous mesh during transition. Responses of PEO electrospun fibrous mesh under different relative humidity was studied as well.

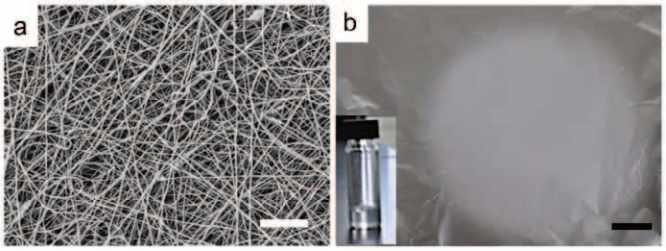

Figure 1 (a) Morphology of electrospun fibers from 4% w/v PEO polymer solution under scanning electron microscopy. The scale bar is 25 micron. (b) Image of 4%w/v electrospun fibrous mesh on aluminium foil with a scale bar of 2 cm. Insert image is approximate 1 mL of PEO solution in a 4 mL glass vial.

Electrospinning technology is a versatile and effective method to fabricate fibers of several tens to hundreds of nanometers diameter from various materials, and PEO is one of the most frequently used materials to produce electrospun fibers[8]. The electrospinning was performed on a home-made electrospinning setup. Our PEO fibrous mesh was produced by electrospinning a 1 mL of 4%w/v PEO solution for 1 hour in humidity controlled cubic chamber at room temperature. A piece of grounded aluminium foil was used as stationary grounded collector. The distance from the tip to the needle is 12 cm and voltage was set at 4 kV during electrospinning. Humidity was monitored by a digital humidity and temperature thermometer during electrospinning and controlled by N_2 gas flow. From the scanning electron microscopy (SEM) images shown in Figure 1(a), we can see clearly fibrous structure. Diameter of electrospun fibers are 0.94±0.20 μm. PEO polymer solution was transparent (Figure 1b insert image), After electrospinning, since light scattering occurs on the interface of air/fiber and the random orientation of fibers, incident light will be blocked, electrospun fibrous mesh appears to be opaque and the color of white (Figure 1b).

After electrospinning process, resulted fibrous mesh was transferred from aluminium foil onto an optical clear adhesive film that is usually for 96 well plate sealing, which has much higher mechanical strength than electrospun fibrous mesh. The diameter of the electrospun mesh is about 9 cm and the sealing film has lightly larger size that is 12 x 9 cm. After the electrospun process, the sticky side of the sealing film was carefully placed from one edge gradually to the other edge to cover entire electrospun fibrous mesh. Thus the entire mesh adhered evenly onto the film. Later whole electrospun fibrous mesh was easily peeled off from aluminium foil without any residuals and cutted into small slices for humidity detection. This even transferring process guarantees the variation of thickness between different small slices is minimum. This composite material was used through all the experiments. For convenience, we will refer this composite materials as electrospun fiber mesh from this point, unless specific indication.

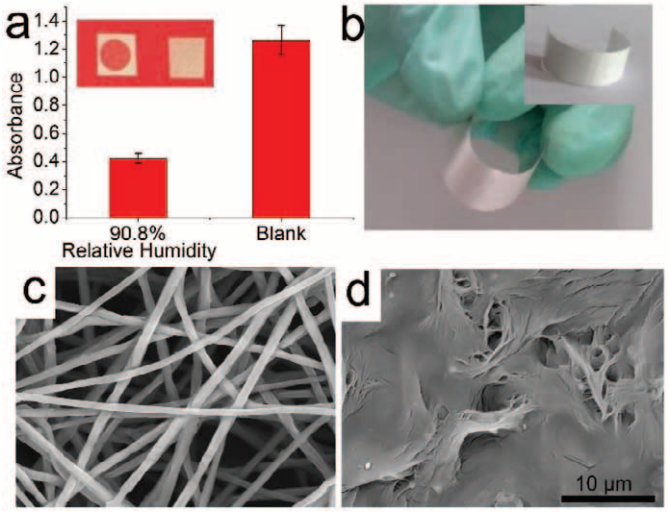

Figure 2. (a) Image (insert image) and absorbance of electrospun fibrous mesh before and after exposure to 90.8% relative humidity. Error bar represented standard deviation (n=3). (b) Flexibility of electrospun fibrous mesh on optical clear single-side adhesive film. (c) and (d) SEM image of electrospun fibers before and after exposure to 90.8% relative humidity, respectively. SEM Images (c) and (d) have the same magnification and scale bar is 10 micron.

The whole electrospun fibrous mesh was cut into about 1x1 cm squares or 1x 6 cm strips. As shown in the images in Figure 2b, our material is flexible and has good mechanical strength which will benefit handling and easy to use in further applications. When a piece of this fibrous mesh was covered on top of a well that contains water in 96 well plate, a round shape transparent spot formed on fibrous mesh as shown in insert photo in Figure 2a. When that photo was taking, Red color paper was placed underneath the fibrous mesh to enhance the contrast. And the absorbance of fibrous mesh at 400 nm decreased accordingly as shown in Figure 2a. SEM image shows much clear view of what is happened. Before exposure to water vapor, fibers can be seen clearly in Figure 2c. After exposure we can see in Figure 2d, almost all of the fiber structure disappeared, however traces of previous fibers still clear. Thus from morphology of remained

structure, we presume it is caused by fusion of the fibers. To confirm our assumption, we examined the morphology of fibrous mesh after different exposure time under SEM.

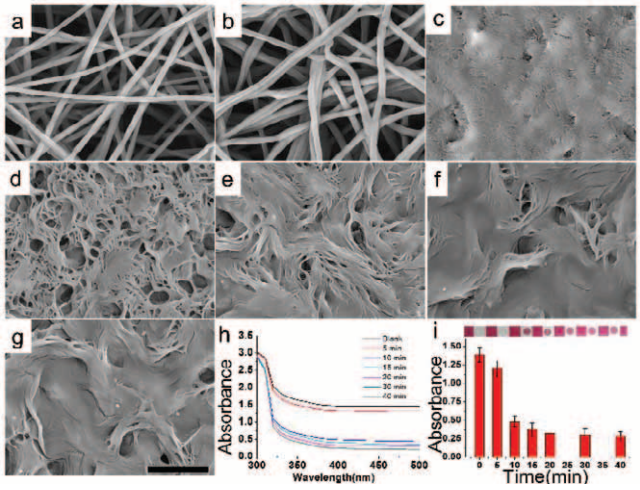

Figure 3 SEM Images of electrospun fibrous mesh before and after expose to 90.8 % relative humidity for a serial of time (a, 0; b, 5; c, 10; d, 15; e, 20; f, 30; g, 40 min). All images have same magnification and the scale bar is 10 micron; UV-vis spectra (h) and absorbance (i) of electrospun fibrous mesh before and after expose to of 90.8% relative humidity for a serial of time. Error bar represented standard deviation (n=3). Insert image in (i) represents the photo of fibrous mesh.

As shown in Figure 3 a-g, comparing with unexposed fibers, after 5 min in 90.8% relative humidity, fibers appear to be slightly curvier than before. Some adjacent fibers are start to shown sign of merging. After 10 min exposure, we can see clearly that fibers melted and fused together to form film like structure. After 15 min exposure, most of fibers are melted together and only trace of fibers can be seen in the image. The holes are apparently from the empty space between fibers. From 20 to 40 min exposure, surface becomes more and more flat and uniform. From figure 3h, we can observe that the absorbance of electrospun fiber mesh decrease as the time increases. From the insert image in Figure 3i, we can see clearly a transparent circle formed after 10 min exposure. For longer time, the transparency of fibrous mesh are similar. Since absorbance is caused by reflection of the random oriented fibrous fibers, it is almost irrelevant to wavelength. Thus we can observe very similar absorbance from 400nm to 600 nm for each kind of fibers in Figure 3h. Namely, any absorbance of each sample from 400 nm to 600 nm could be chose to represent its transparency. To test the reproducibility of this phenomena, we measured the absorbance of all fibrous mesh at 400 nm in triplicates, data was shown in Figure 3i. For 5 min exposure time, we can observe slightly decrease in absorbance. For 10 min exposure, the decrease in absorbance is significant. For longer exposure time, the absorbance decrease lightly until reach a plateau after 20 min.

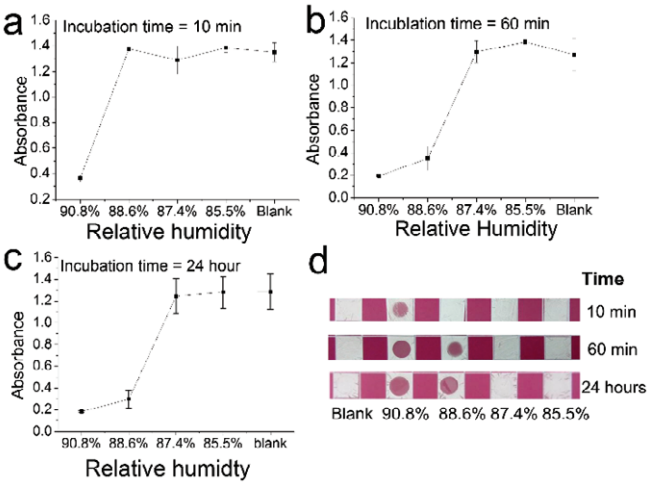

Figure 4 (a-c) Absorbance of electrospun fibrous mesh expose to different relative humidity condition for 10 min, 60 min, 24 hours. (d) Images of electrospun fibrous mesh exposure to different relative humidity condition for different time. Error bar represented standard deviation (n=3).

Based on the results we got so far, we utilized this rapid and stable optical transition of PEO fibrous mesh to sensing high humidity. As shown in Figure 4, if we control the exposure time in less than 10 min, only 90.8% relative humidity can cause transition of opaque to transparent of PEO. If we extend the exposure time to 60 min, transition starts to occur under 88.6% relative humidity. Surprisingly even we extend the exposure time to 24 hours, still only when relative humidity is higher than 88.6% could induce the transition of the fibrous mesh. The unique phenomena would make this pure PEO electrospun fibrous mesh a non-toxic, low cost, and practical "cut-off" sensor for high humidity monitoring in food.

We summarized typical humidity techniques with best RH range reported so far in Table 1, as well as their responsing elements. Since our sensor only compose of a nontoxic polymer, polypolyethylene oxide. Thus it has simplest composition (low cost) and minimum possibility in toxicity among these methods, which are critical for food quality monitoring at each individual package. Although relative humidity range of our methods is narrow, it is quit suitable at the range of moulds and yeasts infest cereals and rice.

Table 1 Summary of humidity detection techniques.

Techniques	Response elements	RH range[a]	Ref.
Amperometry	Polytetrafluorothylene film	20-100%	2a
Capacitance measuring	Silver nanoparticle	35%-90%	2b
Resistance measuring	PEDOT:PSS/Iron Oxide Nanoparticle	20-95%	2c
Voltage measuring	CuTCNQ/ZnO Nano Tube arrays	5-90%	2d
Quartz crystal microbalance	Polyethyleneimine modified polyamide 6 nano-fiber/net	2%-95%.	10b
Fluorometry	Dapoxyl sulfonic acid	3%-96%	3a
Colorimetry	Fe_3O_4 Nanoparticles	11%-97%	7a
	$CoCl_2$	5%-60%	
Current method	Polypolyethylene oxide fibrous mesh	88-90%	

a: RH, Relative humidity

We thank the National Natural Science Foundation of China (Grant No. 21305083), Changjiang Scholars and Innovative Research Team in University (Grant No. IRT 1124), and Fundamental Research Funds for the Central Universities (Grant No. GK201303003 and GK201402051) for financial support.

Conclusions

We studied the transition of electrospun micro/nano fibrous mesh from opaque to transparent by UV-Vis spectroscopy and scanning electron microscopy. We used water soluble and nontoxic polymer polyethylene oxide (PEO) to fabricate electrospun fibers. In the vapor of water, PEO electrospun fibers start to fuse together, which cause the dramatic decrease of air/fiber interfaces. Since the random orientation of fibers, light scattering at the air/fiber interface blocked the light. As the air/fiber interfaces are disappearing, the fibrous mesh become more and more transparent. At room temperature, PEO electrospun fibrous mesh becomes transparent in 10 min under 90.8% relative humidity condition, and takes 60 min for the similar transition in 88.7 % relative humidity. Astonishingly, even we extended the exposure time to 24 hours, the fibrous mesh remains opaque under lightly lower relative humidity 87.4%. Thus pure PEO electrospun fibers can be used as safe, irreversible, equipment-free, and cheap (< \$0.002 per 1x1 cm^2) "cut-off" sensor for high humidity monitoring when low toxicity and irreversible are high required, such as in rice and cereals.

Notes and references

[a] Key laboratory of analytical chemistry for life science of Shaanxi Province, School of Chemistry and Chemical Engineering, Shaanxi Normal University, Xi'an, Shaanxi, 710119, P. R. China. E-mail: duanxr@snnu.edu.cn, lzpbd@snnu.edu.cn

† Electronic Supplementary Information (ESI) available: [Experimental details are presented in Electronic Supporting Information.]

1 H. W. Yu, H. K. Kim, T. Kim, K. M. Bae, S. M. Seo, J. M. Kim, T. J. Kang, and Y. H. Kim, *ACS Appl. Mater. Interfaces* 2014, **6**, 8320

2 (a) H. Guo, J. Chen, L. Tian, Q. Leng, Y. Xi, and C. Hu *ACS Appl. Mater. Interfaces* 2014, **6**, 17184. (b) M. Mraović, T. Muck, M. Pivar, J. Trontelj and A. Pleteršek, *Sensors* 2014, **14**, 13628-13643. (c)S. Taccola, F. Greco, A. Zucca, C. Innocenti, C. de J. Fernández, G. Campo, C. Sangregorio, B. Mazzolai, and V. Mattoli, *ACS Appl. Mater. Interfaces* 2013, **5**, 6324. (d) Ke Wang, Xuemin Qian, Liang Zhang, Yongjun Li, and Huibiao Liu *ACS Appl. Mater. Interfaces* 2013, **5**, 5825−5831 (e) P. Su, C. Wang, *Sensors and Actuators B* 2007, **123**, 1071; (f)S. Hwang, D. Kang, R. S. Ruoff, H. S. Shin, and Y. B. Park, *ACS Nano* 2014, **8**, 6739; (g) T. Munoz, Jr. and K. J. Balkus, Jr. *Chem. Mater.* 1998, **10**, 4114. (h) R. Demir, S. Okur, and M. Şeker *Ind. Eng. Chem. Res.* 2012, **51**, 3309;

3 (a) J. C. Tellis, C. A. Strulson, M. M. Myers, and K. A. Kneas, *Anal. Chem.* 2011, **83**, 928. (b) E. Kim, S. Yeon Kim, G. Jo, S. Kim, and M. J. Park, *ACS Appl. Mater. Interfaces* 2012, **4**, 5179. (c) D. Bridgeman, J. Corral, A. Quach, X. Xian, and E. Forzani, *Langmuir* 2014, **30**, 10785; (d) K. Su1vegh and R. Zelko, *Macromolecules* 2002, **35**, 795

4 (a) M. Beyer, J.-A. Verreet, and W. Ragab, *International Journal of Food Microbiology*, 2005, **98**, 233240. (b) Choi, H. Jun, J. Bang, S.-H. Chung, Y. Kim, B. Kim, H. Kim, L. Beuchat, and J.-H. Ryu, *Food Microbiology*, 2015, **46**, 307313. (c) J. Gilbert, S. M. Woods, and U. Kromer, *Phytopahthology,* 2008, **98**, 504

5 S. Choi, H. Kim, Y. Kim, B. Kim, L. Beuchat, and J.-H. Ryu, *Food Microbiology*, 2014, **38**, 122127.

6 (a) A. Léonard, R. Lauwerys *Mutat. Res-Rev. Genet.* 1990, **239**, 17-27; (b)L. S. Nelson, N. A. Lewin, M. A. Howland, R. S. Hoffman, L. R. Goldfrank, N. E. Flomenbaum Goldfrank's Toxicologic Emergencies. 9th ed. New York, NY: McGraw Hill; 2011. (c) S.J. Stohs, D. Bagchi, *Free Radical Biology and Medicine* 1995, **18**,321

7 (a) H. Hu, Q. Chen, K. Cheng, J. Tang *J. Mater. Chem.*, 2012, **22**, 1021 (b) H. Wang, K. Zhang, *Sensors (Basel)*. 2013, **13**, 4192. (c)N. A. Luechinger, S. Loher, E. K. Athanassiou, R. N. Grass, W. J. Stark, *Langmuir* 2007, **23**, 3473

8 (a) N. Bhardwaj, S. C. Kundu, *Biotech. Adv.* 2010, **28**, 325. (b) D. Li, Y. N. Xia, *Adv. Mater.* 2004, **16**, 1151. (c) A. Greiner, J. H. Wendorff, *Angew. Chem., Int. Ed.* 2007, **46**, 5670

9 C. Zhou, Y. Shi, X. Ding, M. Li, J. Luo, Z. Lu, D. Xiao, *Anal. Chem.* 2013, **85**, 1171

10 (a) W. Zheng, X. Lu, W. Wang, Z. Li, H. Zhang, Z. Wang, X. Xu, S. Li, C. Wang, *J. Colloid Interf. Sci.* 2009, **338**, 366. (b) X. Wang, B. Ding, J. Yu, M. Wang, *J. Mater. Chem.* 2011, **21**, 16231

11 V. O. Sheftel, Indirect Food Additives and Polymers: Migration and Toxicology. CRC Press; 2000.

